



HAL
open science

Effect of Heat Treatment of Carbon Nanofibres on Electroless Copper Deposition

J. Tamayo-Ariztondo, J.M. Córdoba, M. Odén, J.M. Molina-Aldareguia, M.R.
Elizalde

► **To cite this version:**

J. Tamayo-Ariztondo, J.M. Córdoba, M. Odén, J.M. Molina-Aldareguia, M.R. Elizalde. Effect of Heat Treatment of Carbon Nanofibres on Electroless Copper Deposition. *Composites Science and Technology*, 2010, 70 (16), pp.2269. 10.1016/j.compscitech.2010.07.015 . hal-00696567

HAL Id: hal-00696567

<https://hal.science/hal-00696567>

Submitted on 12 May 2012

HAL is a multi-disciplinary open access archive for the deposit and dissemination of scientific research documents, whether they are published or not. The documents may come from teaching and research institutions in France or abroad, or from public or private research centers.

L'archive ouverte pluridisciplinaire **HAL**, est destinée au dépôt et à la diffusion de documents scientifiques de niveau recherche, publiés ou non, émanant des établissements d'enseignement et de recherche français ou étrangers, des laboratoires publics ou privés.

Accepted Manuscript

Effect of Heat Treatment of Carbon Nanofibres on Electroless Copper Deposition

J. Tamayo-Ariztondo, J.M. Córdoba, M. Odén, J.M. Molina-Aldareguia, M.R. Elizalde

PII: S0266-3538(10)00284-8
DOI: [10.1016/j.compscitech.2010.07.015](https://doi.org/10.1016/j.compscitech.2010.07.015)
Reference: CSTE 4769

To appear in: *Composites Science and Technology*

Received Date: 1 March 2010
Revised Date: 8 July 2010
Accepted Date: 17 July 2010

Please cite this article as: Tamayo-Ariztondo, J., Córdoba, J.M., Odén, M., Molina-Aldareguia, J.M., Elizalde, M.R., Effect of Heat Treatment of Carbon Nanofibres on Electroless Copper Deposition, *Composites Science and Technology* (2010), doi: [10.1016/j.compscitech.2010.07.015](https://doi.org/10.1016/j.compscitech.2010.07.015)

This is a PDF file of an unedited manuscript that has been accepted for publication. As a service to our customers we are providing this early version of the manuscript. The manuscript will undergo copyediting, typesetting, and review of the resulting proof before it is published in its final form. Please note that during the production process errors may be discovered which could affect the content, and all legal disclaimers that apply to the journal pertain.



Effect of Heat Treatment of Carbon Nanofibres on Electroless Copper

Deposition

J. Tamayo-Ariztondo^{1*}, J.M. Córdoba², M. Odén², J.M. Molina-Aldareguia³, M.R. Elizalde¹

¹CEIT and Tecnun (University of Navarra). Manuel de Lardizabal 15, 20018 San Sebastián, Spain

²Nanostructured Materials, Department of Physics, Chemistry, and Biology (IFM), Linköping University, 58183 Linköping, Sweden.

³IMDEA-Materiales, c/ Profesor Aranguren s/n, 28040 Madrid (Spain)

ABSTRACT

Cu is a well known heat sink material due to its high thermal conductivity. However, its coefficient of thermal expansion (CTE) is high. One of the most promising solutions for reducing it is to reinforce copper with carbon nanofibres (CNF) because of their low CTE. To exploit the properties of the CNFs a good dispersion of the reinforcement within the matrix must be achieved. One of the processing methods used to obtain a homogeneous CNF distribution is coating the CNF with Cu using electrochemical deposition. In this paper, the effect of the carbon structure on electroless deposition technique is studied. Different CNF have been compared: herringbone (HB), platelet (PL) and longitudinally aligned (previously heat treated) (LAHT). Herringbone and Platelet CNF were heat treated at 2750°C for 30' which resulted in a structure resembling graphite with loops at the fibre surface. These loops are responsible for an enhancement of the copper coating. It is shown that the Cu coverage in electroless deposition is high for the graphene plane and poor at the edges of the plane.

Key words: A. Carbon nanofibres, Copper, Metal Matrix Composites, E. Heat treatment

Acknowledgements:

The financial contribution of EU FP6 031712 INTERFACE project is gratefully acknowledged. The Spanish Government is also acknowledged for the funds received through the Programa Consolider

CSD2006-0053. M.R.E and J.T-A acknowledge the Basque Government (projects Etor tek-inanoGUNE IE08-225 and IE09-243 and project PI-07/17) for the funds received. J.T-A is grateful to the Basque Government for his PhD Grant.

*Corresponding Author. Phone: +34 943212800. E-mail address: jtamayo@ceit.es

ACCEPTED MANUSCRIPT

1. INTRODUCTION

Copper is a material with high thermal conductivity (385 W/mK) and is commonly used in heat sink or heat spreader applications. However, its coefficient of thermal expansion (CTE) is high (16.5 ppm/K) compared to the CTE of materials present in highly thermally loaded devices such as optoelectronic devices, power electronics modules or high-power diode lasers, which are below 10 ppm/K [1].

Carbon nanofibres (CNF) are seen as a good reinforcement for copper in order to reduce the CTE [2]. They also have a high thermal conductivity so potentially the thermal properties of the composite could increase considerably. To fully exploit the properties of the CNF a good dispersion of the reinforcement within the matrix must be achieved and the thermal contact resistance of the interface should be reduced. These nanofibres are vapour grown carbon fibres (VGCF), approximately 100 times smaller than conventional short carbon fibres. This CNF shows thermal conductivities up to 2000 W/mK with reduced coefficient of thermal expansion and are commercially available in kilogram batches at an affordable price [3] comparing to the prices ten years ago. For these reasons they are promising candidates as reinforcement of metal matrix composites.

There have been many attempts to fabricate this type of composite by different routes (liquid infiltration process [4] and electrodeposition [5]), but the main problem is the dispersion of the nanofibres in the whole composite. Electroless plating is a cheap and quick coating technique recently applied to ceramic powders and whiskers [6-8]. It is also a process easy to manipulate and when properly applied yields a good coverage of the three dimensional substrates to be coated.

Carbon fibres, carbon nanofibres and carbon nanotubes have been coated by electroless copper deposition before [3, 9-12]. In these cases, a hard chemical treatment of the surface of the carbon nanofibres was needed to achieve uniform coverage [9, 12]. Further improvement of the density of the copper coating can be achieved with a subsequent heat treatment step [10].

This paper reports the effect of a high temperature heat treatment (2750 °C) of different types of carbon nanofibres prior to the electroless Cu deposition process. Three types of carbon nanofibres have been studied, with the following structures before the high temperature heat treatment: platelet, herringbone and longitudinal aligned structures. High temperature heat treatments of carbon nanofibres and carbon nanotubes result in structural changes both internally and at the surface [13-18]. For example, heat treating carbon nanofibres at temperatures above 2200 °C results in a high degree of graphitization [16]. In this study the structure and chemical state of the fibers have been analyzed by transmission electron microscopy (TEM) and infrared spectroscopy (FTIR) and the quality of the Cu coatings by scanning electron microscopy. It is shown that the high temperature heat treatment results in improved Cu coatings and the origins of this are discussed.

2. EXPERIMENTAL PROCEDURE

The following nanofibres have been studied: as received herringbone (HB), heat treated herringbone (HBHT), as received platelet (PL), heat treated platelet (PLHT) and longitudinally aligned (previously heat treated) (LAHT). Herringbone and platelet carbon nanofibres were acquired from Future Carbon GmbH, Germany, while longitudinally aligned carbon nanofibres were acquired from Showa Denko Inc, Japan. These types of nanofibres have been described in previous works [18-20].

CNF HB and PL from Future Carbon GmbH have been heat treated while LA is already subjected to a final heat treatment at high temperature during fabrication. The heat treatment of HB and PL was performed in a graphitization furnace (Thermal Technology Inc. - max. temperature: 2900 °C) at 2750 °C for 30 minutes in a helium atmosphere. Temperature was increased at 20 °C/min up to 850 °C, followed by a heating rate of 10 °C/min up to 2750 °C. After the 30 min plateau, the cooling was made following the same schedule as for heating.

Then, electroless plating was performed with both heat treated and as received carbon nanofibres. The following steps are needed for electroless plating: surface treatment, sensitization, activation and deposition. In this work the same process parameters have been used to coat the different CNF except in the case of the surface treatment where two different reagents have been used. All the process steps were conducted in an ultrasonic bath at room temperature (Model B-5510MTH, 40 kHz transducers, Branson).

Surface treatment of the CNF is the first step. It is needed for cleaning the surface and creating anchor points on the CNF surface [11]. These anchor points are functional groups. The functional groups that appear in the CNF are: hydroxyl (O-H), carboxylic (C=O) and carbonylic (C-O). These functional groups present covalent bonding at the edges and structural defects of the fibers [21]. Two different surface treatments were used: H₂SO₄ and boiling acetone plus H₂SO₄/K₂Cr₂O₇. The treatment with sulphuric acid is softer than the one with boiling acetone plus sulphuric acid with potassium dichromate.

Sensitization of the CNF was achieved with a solution of SnCl₂ with HCl and activation with a solution of PdCl₂ with HCl, both in distilled water. These steps are

necessary for the subsequent reactions during electroless plating. In Table 1 amounts and reaction time of each solution are shown.

Finally, electroless plating was executed for thirty minutes. Details of the bath composition are shown in Table 2. Working conditions were pH = 12 and room temperature.

The structure of HB, HBHT, PL, PLHT, and LAHT has been characterized by TEM (FEI Tecnai G2 TF 20 UT microscope operated at 200 kV). TEM samples have been prepared by dispersing the carbon nanofibres in ethanol and depositing them onto a hollow carbon grid. The structure of the CNF has been compared with the structure of graphite powder ($\text{Ø} < 20 \text{ }\mu\text{m}$, synthetic, Aldrich) [9]. Interplanar d-spacings were determined by X-ray diffractometry (XRD) performed on a Philips PW1729 X-ray diffractometer using Cu K α radiation.

The anchor points obtained in the surface treatment step have been analyzed by FTIR (Bruker Vertex 70). The analysis has been done for carbon nanofibres (HB, PL, HBHT, PLHT and LAHT) and graphite (graphite is used as a standard) without surface treatment and with the two types of surface treatments performed: H $_2$ SO $_4$ and boiling acetone plus H $_2$ SO $_4$ with K $_2$ Cr $_2$ O $_7$.

The surface specific area of the carbon nanofibres and the graphite has been measured by Brunauer-Emmett-Teller (BET) analysis (Micromeritics: ASAP 2020). The measurements have been made on as received CNF, heat treated CNF and as received and heat treated CNF after the hardest surface treatment (boiling acetone plus H $_2$ SO $_4$ /K $_2$ Cr $_2$ O $_7$).

Finally, the quality of the copper coating on the CNF has been studied using SEM (LEO 1550 Gemini). The coating of as received and heat treated herringbone and

platelet CNF have been compared after both surface treatments. Also, longitudinally aligned CNF have been coated and analyzed by SEM.

3. RESULTS AND DISCUSSION

Figure 1 shows the structure of the HB nanofibre before and after the heat treatment at 2750°C for 30 minutes. The graphene layers show a preferred orientation but the stacking is not regular (fig 1 (a)). Once heat treated (fig 1 (b)) the graphene layers are parallel to each other. The heat treated carbon nanofibres have a structure very similar to graphite (see Fig. 1(c)) as the distance between the graphene layers in both micrographs is nearly the same (3.37 Å for HBHT and 3.35 Å for graphite). The graphitization of VGCF after a heat treatment at temperatures above 2200°C has been observed in previous work [16]. Note that the fibre surface is modified: loops of graphene appear to have joined the graphene layers edges. These loops have been reported in previous studies [16, 22-24]. Lee et al. suggested loops to appear at 2200 °C, however, not very clearly shown [16]. Endo et al. observed developed loops when the nanofibres were heat treated at 3000°C [22]. This work shows that distinct loops have developed already at 2750°C. These loops might be formed by a zipping mechanism which gives a structural stability to heat treated nanofibres [22].

In the case of PL (Fig. 1(e)), the change of the structure is not as pronounced as for the HB-CNFs, although the distance between graphene sheets in PLHT is 3.37 Å (fig. 1(f)), approaching the distance in graphite. Similarly to HBHT, loops are also seen at the outer graphene layers of PLHT. The degree of crystallinity of the CNF appears to be high, in agreement with Pacault et al., who found out that the graphitization degree is not very dependent on the time but on the temperature of the heat treatment [25].

Figure 1(d) shows a HR-TEM micrograph of the LAHT. The distance between the graphene layers is 3.37 Å and the graphene layers are parallel to the nanofibre axis.

Figure 2 shows FTIR analysis of LAHT, HB, HBHT, PL, PLHT and graphite prior and after different chemical surface treatments. The spectra contain peaks corresponding to the expected functional groups, which include O-H groups ($\sim 2900\text{ cm}^{-1}$), C=O groups ($\sim 1670\text{-}1760\text{ cm}^{-1}$) and C-O groups ($\sim 1000\text{-}1200\text{ cm}^{-1}$) [7]. These functional groups make a covalent bonding with the carbon nanofibres. The peaks found at 3400 cm^{-1} and at 2400 cm^{-1} refer to H_2O and CO_2 , respectively. These molecules appear as soon as the sample is exposed to air (Figure 2).

Comparing figures 2(a) and 2(b) it can be observed that for the soft surface treatment (H_2SO_4) only LAHT, PL, PLHT and, over all, graphite show functional groups. PL and PLHT have small peaks in the O-H and graphite and LAHT show clear peaks in the three zones expected. When the chemical treatment is harder (boiling acetone + $\text{K}_2\text{Cr}_2\text{O}_7/\text{H}_2\text{SO}_4$), all the carbon nanofibres have significant peaks except the as received HB, as shown in figure 2(c).

Regarding the effect of the heat treatment, in general, the heat treated PL displays the same peaks than the as-received PL. However this is not true in the case of HB with a hard chemical treatment where clear peaks associated with the C-O and C=O groups appear only for the heat treated HB, while as-received HB CNFs show no reactivity whatsoever.

The different surface area values of the carbon nanofibres after surface treatment and heat treatment were compared with the values of the as received CNF. Table 3 shows all the values measured by BET. The chemical treatment with which the surface area of the CNF has been measured was boiling acetone plus $\text{H}_2\text{SO}_4/\text{K}_2\text{Cr}_2\text{O}_7$. The

percentage of surface area loss means the loss of surface area in HBHT, PLHT, graphite and LAHT before and after the chemical treatment.

The value of the surface area is reduced considerably when the HB is heat treated whereas the surface area reduction, although significant, is smaller after the heat treatment in the case of PL CNFs. This fact could be because the smallest CNFs, which are those that give high values of surface area, are vaporized at high temperature and disappear. Therefore, the mean diameter is larger and as a result the surface area is reduced. The surface area also decreases during the heat treatment because contaminations are removed.

In the case of HB, the surface area decreases significantly after the surface treatment. However this does not occur for the HBHT, PL and PLHT, where the surface area reduction after the surface treatment is small. This is related to the large disorder of as-received HB CNFs, which display a large local roughness, as can be seen in figure 1 (a). On the contrary, the rest of the nanofibres studied have a very smooth surface and do not suffer significant surface area changes after the surface treatment.

From the percentage of surface area loss it can be noticed that the percentage of surface area loss in HBHT, PLHT, graphite and LAHT after the chemical treatment is similar. This means that they have similar behaviour when they are exposed to the same surface treatment.

Concerning the electroless plating, the SEM micrographs show that herringbone nanofibres with a chemical treatment of H_2SO_4 (Figure 3 (a)) are barely coated by copper, as it was also shown elsewhere [9]. However, heat treated CNFs with the same chemical treatment (Figure 3 (b)) are coated to a high percentage. Concerning the PL, Cu was not deposited in the as received CNFs (fig 3(c)), whereas in the heat treated (fig.

3(d)) it was barely deposited. Moreover, the small amount of copper found was deposited in clusters.

In the case of the hardest chemical treatment made with boiling acetone plus $\text{H}_2\text{SO}_4/\text{K}_2\text{Cr}_2\text{O}_7$ all types of CNF tested show some Cu deposition. In the case of herringbone CNFs, both as received and heat treated CNF have been properly coated as can be observed in figure 3(e) and 3(f), respectively. However, the heat treated ones were coated in a more dense and uniform way while the not treated ones seem to be coated in grains. PL was poorly coated (fig. 3(g)) and heat treatment only improved it marginally (PLHT, fig 3(h)), i.e. copper was deposited but in the form of agglomerates.

Finally, in the case of LAHT (figure 4), a dense and uniform coating was obtained. The structure of the LAHT fibres seen by TEM seems to be very good for electroless Cu deposition, providing the dense coating seen in figure 4. This indicates that when the graphene layers are longitudinally aligned, Cu coverage during electroless coating is the best.

In summary, provided that the right surface treatment is used for functionalisation, it is possible to deposit Cu on all types of CNF tested. However, the quality of the Cu coating is very dependent on the structure of the CNF. The densest Cu coating is obtained in LAHT, with its graphene layers oriented parallel to nanofibre axis. However, as received PL and HB, with a low degree of crystallinity and with the graphene layers perpendicular to the fibre axis display poor Cu coverage, especially those in which graphene layers meet the surface perpendicularly (i.e. PL, see fig. 1(e)). The high temperature treatment improves the quality of the Cu coating dramatically, especially in the case of HBHT. This is related to the graphitisation of the CNF and the formation of graphene loops at the surface, providing a good surface for electroless

coating, similar to that encountered in LAHT. Some improvement on the deposited Cu is also observed in the PLHT, but in this case the Cu deposited is less dense, showing more agglomerates.

In addition, the results show that, although the functionalisation of the CNFs is critical to create anchor points for the coating process to begin; this is by itself not enough to produce a good coating, as shown in the case of the PL. For a good dense coating to form, the graphene layers must be parallel to the surface of the CNF as shown for LAHT and HBHT. A likely scenario is that palladium is bound to the fibres through the functional groups during the activation step. The Cu deposition is then initiated at those points and progresses along the fibre surface until full coverage is reached. This can be observed in Figure 5, where the coating process in the bath is interrupted after 5 minutes for LAHT-CNFs. Functional groups form covalent bonds with graphene and hence appear at the fibre edges and at defects along the LAHT-CNF surface. It can be seen that Cu nucleates at these points. Once the oxidation-reduction starts its expansion along the fibres is favoured when the graphene layers are oriented parallel to the fibre surface.

4. CONCLUSIONS

It has been shown that a heat treatment at 2750 °C during 30 minutes graphitizes the herringbone and platelet carbon nanofibres. Surface area decreases drastically after the heat treatment for herringbone CNF, because the nanofibres with the smallest diameter are vaporized and disappear. It is also shown that after a surface treatment, the percentage of surface area loss in HBHT and PLHT, as well as in graphite and LAHT, is similar.

Heat treated CNFs show a higher reactivity for electroless Cu coating, requiring softer chemical treatments than as-received CNFs. This occurs because the heat treatment induces the formation of graphene loops at the surface of the CNFs.

The best coating was obtained with longitudinally aligned carbon nanofibres, as well as heat treated herringbone CNF, which show a really dense and uniform coating after a surface treatment with boiled acetone plus $H_2SO_4/K_2Cr_2O_7$ solution. This is related to the favourable orientation of the graphene layers at the surface of the nanofibres. On the contrary, platelet carbon nanofibres, with graphene layers perpendicular to the fibre surface, were not as well coated, even if anchor points were formed after the surface treatments. In summary, under electroless copper deposition, Cu deposits preferably on those surfaces parallel to graphene layers, due to the exposure of π bonds in the outer surface, and deposition is inhibited on surfaces perpendicular to the graphene layers.

5. REFERENCES

1. Schrank C, Eisenmenger-Sittner C, Neubauer E, Bangert H, Bergauer A. Solid state de-wetting observed for vapor deposited copper films on carbon substrates. *Thin Sol Fil* 2004; 459: 276–281.
2. Dong S R, Tu J P, Zhang X B. An investigation of the sliding wear behaviour of Cu-matrix composite reinforced by carbon nanotubes. *Mat Sci Eng* 2001; 313: 83–87.
3. Barcena J, Maudes J, Coletto J, Baldonado J L, Gomez de Salazar J M. Microstructural study of vapour grown carbon nanofibre/copper composites. *Comp Sci Tech* 2008; 68 1384-1391.
4. Younghwan J, Sangshik K, Sangkwan L, Doohyun K, Moonkwang U. Fabrication of carbon nano-sized fiber reinforced copper composite using liquid infiltration process *Comp Sci Tech* 2005; 65: 781–784.

5. Arai S, Endo M. Carbon nanofiber–copper composite powder prepared by electrodeposition. *Elec Comm* 2003; 5: 797–799.
6. Sharma R, Agarwala R C, Agarwala V. Development of copper coatings on ceramic powder by electroless technique. *Appl Surf Sci* 2006; 252: 8487-8493.
7. Ling G P, Li Y. Influencing factors on the uniformity of copper coated nano-Al₂O₃ powders prepared by electroless plating. *Mat Lett* 2005; 59: 1610-1613.
8. Chang S Y, Lin S J. Fabrication of SiCw reinforced copper matrix composite by electroless copper plating. *Scr Mat* 1996; 35-2: 225-231.
9. Córdoba J M, Odén M. Growth and characterization of electroless deposited Cu films on carbon nanofibers. *Surf Coat Tech* 2009; 203: 3459–3464.
10. Kim I S, Lee S K. Fabrication of carbon nanofiber/Cu composite powder by electroless plating and microstructural evolution during thermal exposure *Scr Mat* 2005; 52: 1045–1049.
11. Wang F, Arai S, Endo M. Metallization of multi-walled carbon nanotubes with copper by an electroless deposition process. *Elec Comm* 2004; 6: 1042–1044.
12. Jahazi M, Jalilian F. The influence of thermochemical treatments on interface quality and properties of copper/carbon-fibre composites. *Comp Sci Tech* 1999; 59: 1969-1975.
13. Endo M, Takeuchi K, Kobori K, Takahashi K, Kroto H W, Sarkar A. Pyrolytic carbon nanotubes from vapor-grown carbon fibers. *Carbon* 1995; 33-7: 873-881.
14. Paredes J I, Burghard M, Martínez-Alonso A, Tascón J M D. Graphitization of carbon nanofibers: visualizing the structural evolution on the nanometer and atomic scales by scanning tunneling microscopy. *Appl Phy* 2005; A80: 675-682.

15. Bougrine A, Dupont-Pavlovsky N, Naji A, Ghanbaja J, Marêché J F, Billaud D. Influence of high temperature treatments on single-walled carbon nanotubes structure, morphology and surface properties. *Carbon* 2001; 39: 685–695.
16. Lee S, Kim T R, Ogale A A, Kim M S. Surface and structure modification of carbon nanofibers. *Synth Met* 2007; 157: 644–650.
17. Córdoba J M, Tamayo-Ariztondo J, Molina-Aldareguia J M, Elizalde M R, Odén M. Morphology influence of the oxidation kinetics of carbon nanofibers. *Corr Sci* 2009; 51: 926–930.
18. Jung A, Jess A, Schubert T, Schütz W. Performance of carbon nanomaterial (nanotubes and nanofibres) supported platinum and palladium catalysts for the hydrogenation of cinnamaldehyde and of 1-octyne. *App. Cat. A*; 2009; 362: 95-105.
19. Jess A, Kern C, Schrögel K, Jung A, Schütz W, *CIT* 2006; 78: 94–100.
20. Endo M, Kim Y A, Hayashi T, Nishimura K, Matusita T, Miyashita K, Dresselhaus M S. Vapor-grown carbon fibers (VGCFs) Basic properties and their battery applications *Carbon* 2001; 39: 1287–1297.
21. Gogotsi Y, Functionalization of Carbon Nanotubes, in *Nanotubes and Nanofibers*, Taylor and Francis Group, 2006, 42-43.
22. Endo M, Kim Y A, Hayashi Y, Yanagisawa T, Muramatsu H, Ezaka M, Terrones H, Terrones M, Dresselhaus M S. Microstructural changes induced in “stacked cup” carbon nanofibers by heat treatment. *Carbon* 2003; 41: 1941–1947.
23. Yoon S H, Park C W, Yang H, Korai Y, Mochida I, Baker R T K, Rodriguez N M. Novel carbon nanofibers of high graphitization as anodic materials for lithium ion secondary batteries. *Carbon* 2004; 42: 21–32.

24. Kiselev N A, Sloan J, Zakharov D N, Kukovitskii E F, Hutchinson J L, Hammers J, Kotonosov A S. Carbon Nanotubes from Polyethylene Precursors: Structure and Structural Changes Caused by Thermal and Chemical Treatment Revealed by HREM. *Carbon* 1998; 36: 1149- 1157.

25. Pacault A. The Kinetics of Graphitization, in *Chemistry and physics of carbon*, P L Walker, Editor, 1971, Marcel Dekker Inc: New York, 107-154.

Figure captions

Fig. 1. TEM images of: (a) HB-as received, (b) HB-heat treated, (c) graphite. (d) LA, (e) PL-as received and (f) PL-heat treated.

Fig. 2. FTIR analysis of different types of CNF (LA, HB, HBHT, PL, PLHT) and graphite, (a) without chemical treatment, (b) chemically treated with H_2SO_4 and (c) chemically treated with boiled acetone plus $K_2Cr_2O_7/H_2SO_4$

Fig. 3. SEM micrographs of Cu coated CNFs with chemical treatment of H_2SO_4 : (a) HB-as received, (b) Hb-heat treated, (c) PL-as received and (d) PL-heat treated, and with chemical treatment of boiled acetone plus $K_2Cr_2O_7/H_2SO_4$: (e) HB-as received, (f) HB-heat treated, (g) PL-as received and (h) PL-heat treated

Fig. 4. SEM micrographs of Cu coated LA with chemical treatment of boiled acetone plus sulphuric acid and potassium dichromate

Fig. 5. SEM micrographs of Cu coated LA with chemical treatment of boiled acetone plus sulphuric acid and potassium dichromate with 5 minutes of electroless: (a) general overview; (b) detail of (a). (Nucleation zones in white circles)

Table 1. Sensitization and activation before electroless plating [7]

	Agent	Concentration	Time (min)
Sensitization	SnCl ₂ * 2H ₂ O	0.04 M	5
	HCl	40 ml/l	
Activation	PdCl ₂	7 * 10 ⁻⁴ M	5
	HCl	2.5 ml/l	

ACCEPTED MANUSCRIPT

Table 2. Composition of the electroless bath solution [7]

Agent	Formula	Role in bath solution	Concentration
Cupric sulphate	$\text{CuSO}_4 \cdot 5\text{H}_2\text{O}$	Coating ions (Cu^{2+})	0.1 M
Rochelle Salt	$\text{C}_4\text{H}_4\text{O}_6\text{NaK} \cdot 4\text{H}_2\text{O}$	Complexing agent	0.2 M
Sodium hydroxide	NaOH	Buffering solution	0.5 M
Formaldehyde	HCHO	Reducing agent	17.5 ml/l

Table 3. Surface area values for the different CNF and graphite

CNF Type	Surface area values (m ² /g)				% Surface area loss in Chemical Treatment
	As received	Chemical Treatment	Heat treatment	Chemical & Heat treatment	
HB	164.81	115.23	22.4	20.89	5.91
PL	72.43	72.16	51.09	48.08	8.4
LAHT	-	-	12.93	11.95	7.62
Graphite	10.81	9.91	-	-	6.74

HB, Herringbone; PL, Platelet; LAHT, Longitudinally aligned

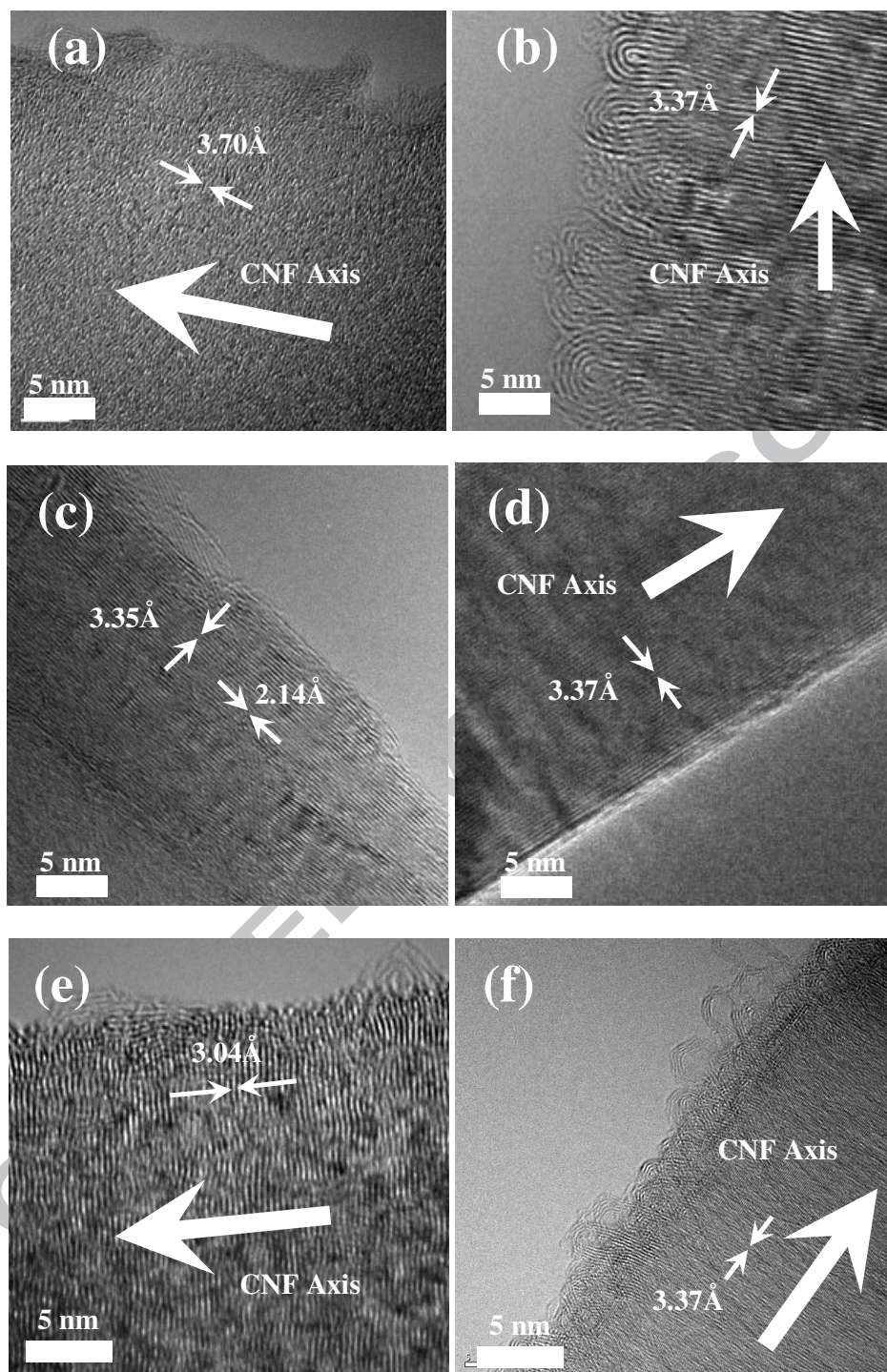


Figure 1

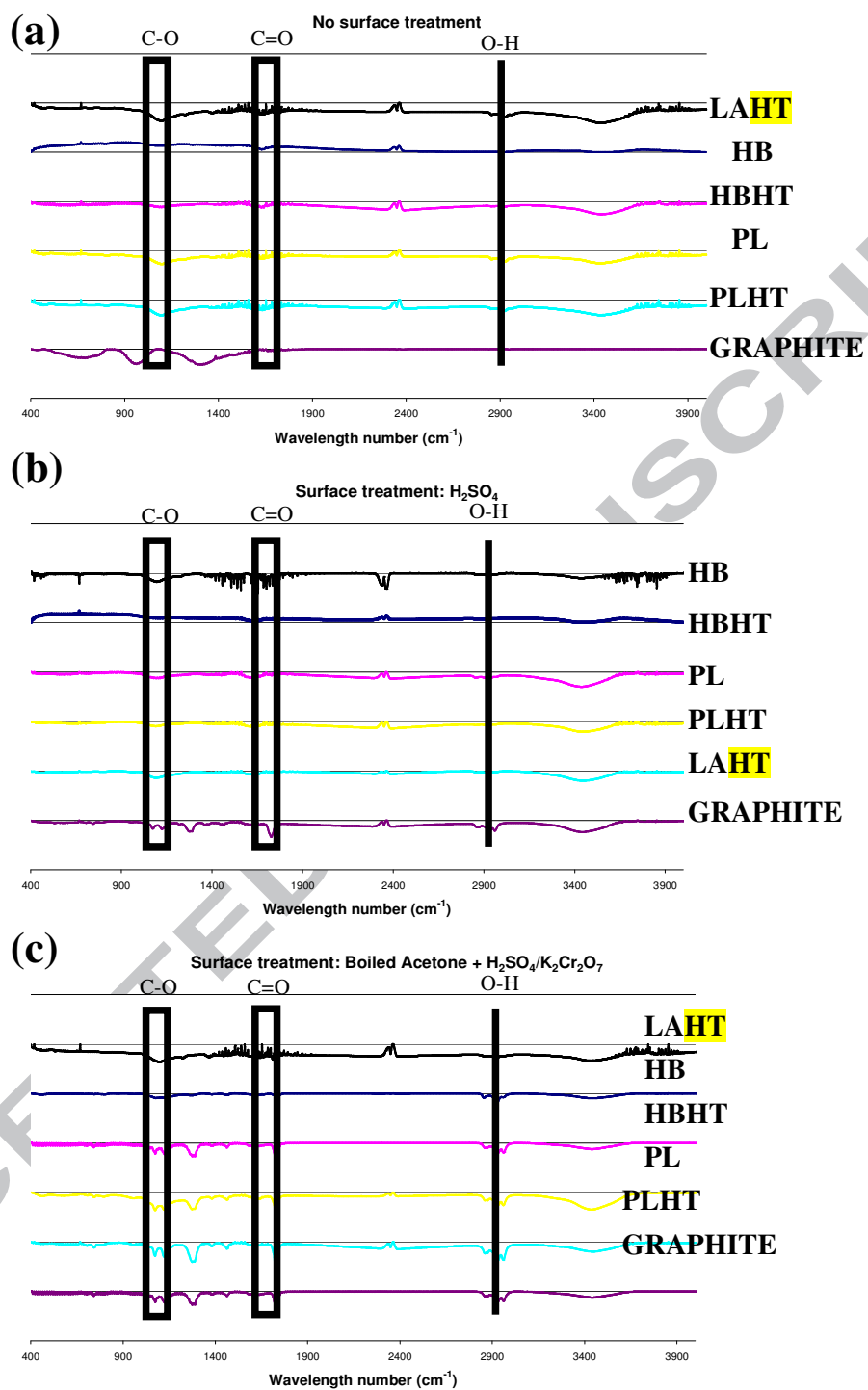


Figure 2

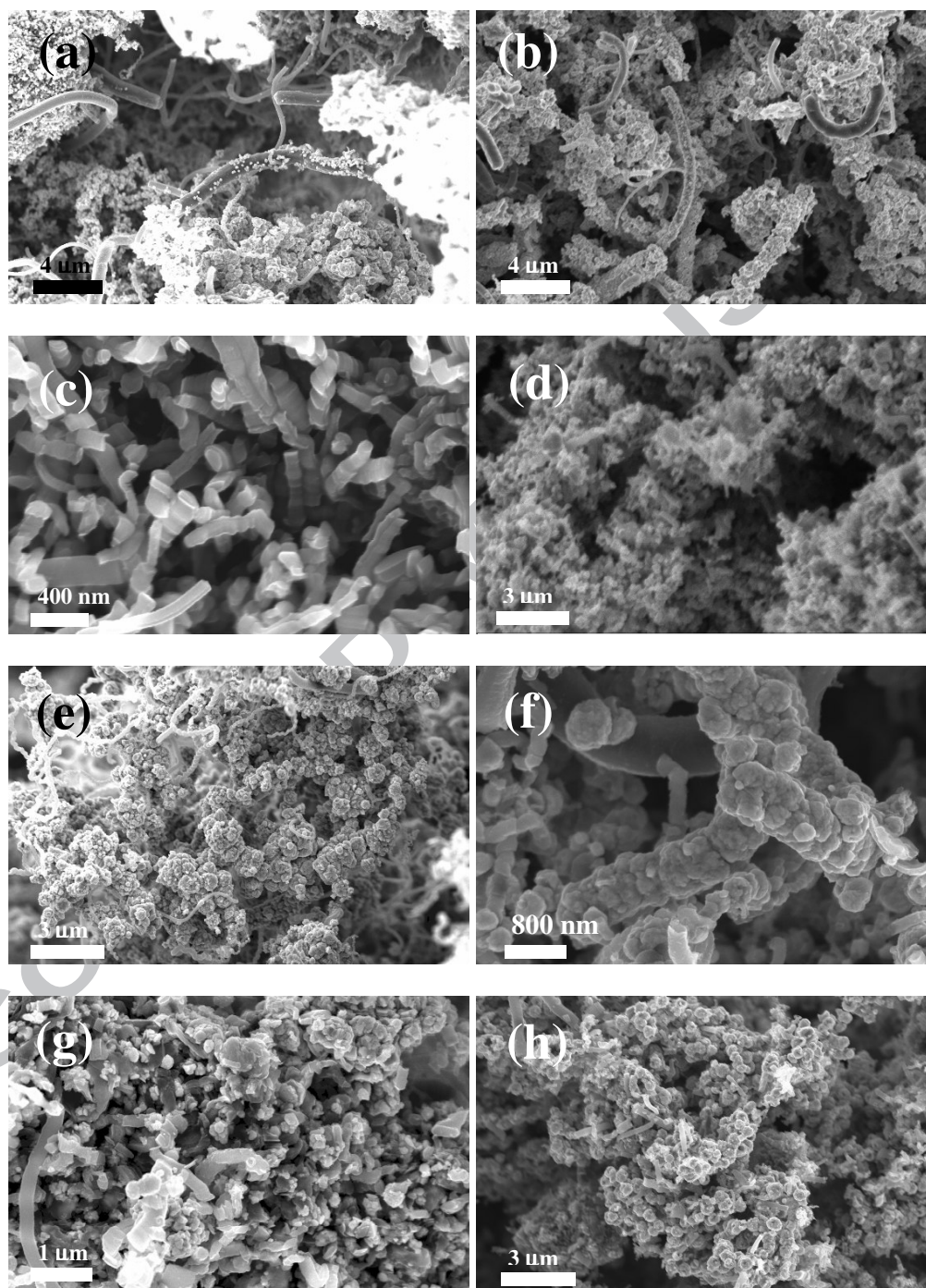


Figure 3

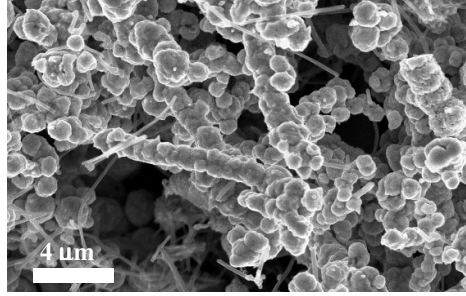


Figure 4

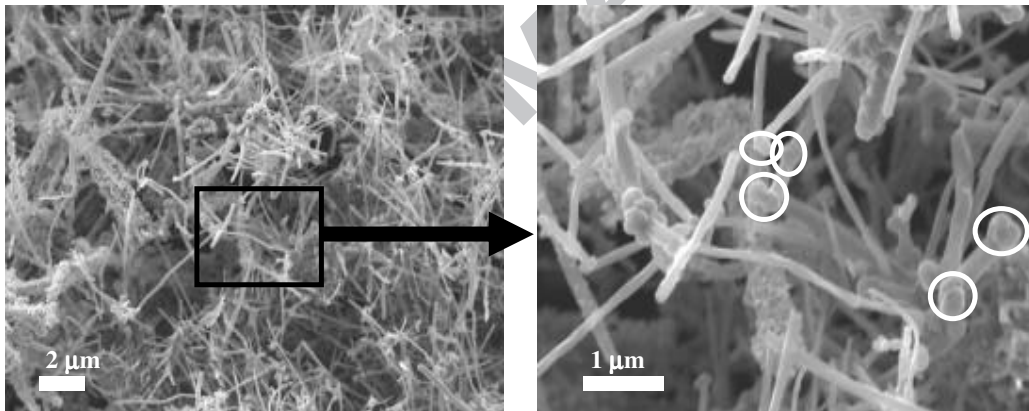


Figure 5